Copyright Warning & Restrictions

The copyright law of the United States (Title 17, United States Code) governs the making of photocopies or other reproductions of copyrighted material.

Under certain conditions specified in the law, libraries and archives are authorized to furnish a photocopy or other reproduction. One of these specified conditions is that the photocopy or reproduction is not to be "used for any purpose other than private study, scholarship, or research." If a, user makes a request for, or later uses, a photocopy or reproduction for purposes in excess of "fair use" that user may be liable for copyright infringement,

This institution reserves the right to refuse to accept a copying order if, in its judgment, fulfillment of the order would involve violation of copyright law.

Please Note: The author retains the copyright while the New Jersey Institute of Technology reserves the right to distribute this thesis or dissertation

Printing note: If you do not wish to print this page, then select "Pages from: first page # to: last page #" on the print dialog screen

ABSTRACT

A mathematical model based on the flow hydrodynamics is developed to calculate the treatment efficiency of ultrafiltration process. This model relates the treatment efficiency with the consideration of both fixed parameters and variable parameters. The fixed parameters are function of the intrinsic rejection coefficient, diffusion coefficient, and viscosity whereas the variable parameters can be related to the fluid velocity, volume flux, and cartridge dimensions. The model has been examined by solutions with solutes that have different molecular weights. The experimental data fits the proposed mathematical model very closely suggesting its suitability to evaluate the rejection efficiency in ultrafiltration. As such the mathematical model can be used to evaluate the intrinsic rejection coefficient that can be used to determine the solvent flux in Kedem Katchalisky model. The role of the particle size is investigated by using a log -log plot of the intrinsic rejection coefficient and the solute molecular weight. Results shows that modeling of the intrinsic rejection coefficient as log normal probability distribution function is possible. Fluid velocity on the membrane cartridge as an important parameter in the design of ultrafiltration systems.

THE INFLUENCE OF HYDRODYNAMICS AND PARTICLE SIZE ON THE REJECTION PROPERTIES OF ULTRAFILTRATION MEMBRANES

by
Usama M. Shahin

A Thesis
Submitted to the Faculty of
New Jersey Institute of Technology
in Partial Fulfillment of the Requirements of the Degree of
Master of Science in Environmental Engineering

Department of Civil and Environmental Engineering

October 1994

APPROVAL PAGE

Hydrodynamics, and Particle Size
Implications on the Rejection Properties of Ultrafiltration Membranes.

Usama M. Shahin

Dr. Spillers, William — Date
Professor and Chairman of Civil and Environmental Engineering, NJIT

Dr. Paul Chan, Committee Member — Date
Professor of Civil and Environmental Engineering, NJIT

Professor: Paul Cheremisinoff, Committee Member — Date
Professor of Civil and Environmental Engineering, NJIT

BIOGRAPHICAL SKETCH

Author: Usama Mohammed Shahin

Degree: Master of Science in Environmental Engineering

Date: October 1994

Undergraduate and Graduate Education

- Master of Science in Environmental Engineering
  New Jersey Institute of Technology,
  Newark, New Jersey, 1994

- Bachelor of Science in Civil Engineering
  Beir-Zeit University,
  Rammalla, West Bank, 1988

Major: Environmental Engineering

This thesis is dedicated to my mother and wife
for their support, and patience

ACKNOWLEDGMENT

The author would like to express his sincere gratitude and appreciation for the guidance and advice given by Dr. William Spillers Professor and Chairman of the Department of Civil and Environmental Engineering at NJIT.

The author would like to thank Dr. Paul Chan Professor of Civil and Environmental Engineering , NJIT. for his constant encouragement and enthusiasm that bolstered the morale of the author during the difficult times, and for serving as a committee member.

Special thanks to Paul Cheremisinoff Professor of Civil and Environmental Engineering , NJIT for his valuable comments, guidance and serving as members of the committee.

The author would like express his indebted to the AMIDEAST and the United States Information Agency for their financial support of the author's graduate study through the FULBRIGHT scholarship.

Last but not least, he thanks his wife and mother for moral support.

TABLE OF CONTENTS

LIST OF TABLES

Table Page

LIST OF FIGURES

CHAPTER 1

INTRODUCTION

1.1 Definition

Filtration is a separation process that is used to separate one or more components from a fluid stream [21, 22]. In membrane filtration the separation process is accomplished using a differential driving potential across a membrane that has selective permeability, physical differences among solution components influence the retention or transport through the membrane [5]. Ultrafiltration (UF) is a pressure driven membrane separation process that uses molecular size differences to separate macromolecules and colloidal matter from solvents and smaller solutes[3].

The differential driving potential used to transport solvent across ultrafiltration and reverse osmosis (RO) membranes is the hydrostatic pressure. The difference between the two processes is the applied pressure range, UF is a low pressure process usually less than 10 atm. while RO operates at pressures above 40 atm [14].

The particle size range for ultrafiltration technology applications extends from 10 A° to 200 A° and roughly corresponds to a molecular weight range from 500 to 500000 amu. On the other hand RO is used to separate molecules as small as ionic species in size. The effective size range of ultrafiltration overlaps the upper end of reverse osmosis and the lower end of microfiltration [3, 5].

1.2 Overview of the problem

The primary environmental engineering application of ultrafiltration systems is to characterize or remove pollutants from water or wastewater [10]. This technology

is becoming increasingly popular as an alternative to conventional treatment processes for water and wastewater treatment [20].

Several analytical methods exist for characterization of pollutants by molecular weight including size exclusion chromatography, field flow fractionation, and ultrafiltration [14, 10]. UF is a relatively inexpensive, nondestructive, and reagent free technique for fractionation of macromolecules. A particular advantage of UF technique is its ability to process relatively large sample volumes [10].

Although ultrafiltration has been available for over a century, it's design is still highly empirical [15]. The complex combinations of hydrodynamics, electrostatic, and thermodynamic forces that control the process have complicated the development of useful mathematical models [15]. Pilot plant and often intermediate sized plants are required to facilitate the design of full scale plants. The understanding of scientific principles is of paramount importance for efficient design and satisfactory management of the treatment facility [15].

Ultrafiltration membranes remove particles from their dispersing media through three distinct mechanisms: primary adsorption, blocking, and sieving. Primary adsorption is dependent on the physicochemical properties of the solution and membrane material, while blocking and sieving are controlled by the solute size relative to membrane's pore diameter. Adsorption and blocking mechanisms are highly unfavorable in ultrafiltration because of their adverse affect on solvent flux and subsequent membrane fouling. Since the goal of ultrafiltration is sieving, adsorption and blocking should be prevented as completely as possible. Asymmetric membranes are characterized by a thin skin layer on the membrane surface [3]. These membranes tend to reduce adsorption and blocking, and therefore sieving is the predominant mechanism in ultrafiltration process using asymmetric membranes [3]. Considering

ultrafiltration as a sieving process, it is important to examine the membrane's separation capability and evaluate the role of system hydrodynamics on solute transport across the membrane under controlled conditions [3].

Membrane manufacturers have adopted the challenge test to define membrane effectiveness. The purpose of this test is to delineate nominal molecular weight cut-off based on specific percent rejection [3]. In this test, the permeability of selected solutes of different molecular weights are measured using a stirred batch cell under controlled operating conditions. The validity of this procedure depends on the solutes employed. Ideally, the solutes should be water soluble, and should represent a range of molecular weights that is consistent with the range of expected rejection coefficients. The solute selection procedure, and the experimental conditions and apparatus hydrodynamics are not standardized among manufacturers [3]. Thus comparison of membrane ratings for different types of molecules or membranes can provide inconsistent results [3].

When water permeates selectively through a membrane, the retained solute accumulates at the solution membrane interface [17]. The solute is then transported back from the membrane by diffusion and consequently a concentration gradient is formed within the boundary layer [18]. This phenomena is termed concentration polarization [3]. It is remarkable to note that no matter what the nature of flow past the membrane, or the feed solution concentration, there always a higher solute concentration in the membrane vicinity than in the feed solution or in the ultrafiltration cell far away from the membrane face [11]. The presence of a concentration boundary layer changes the transport properties of the solute and solvent due to a decrease in the effective differential potential across the membrane [7, 11]. It is also recognized that the

concentrated boundary layer is responsible for discrepancies between apparent and intrinsic membrane reject [7, 11].

1.3 Research objectives

The overall purpose of this research is to conduct a comprehensive analysis of specific membrane rejection properties. There are four primary objectives:

1. Develop a mathematical model to compute the rejection efficiency of ultrafiltration membranes in terms of solution properties and fluid hydrodynamics.
2. Evaluate the solute rejection efficiency of different molecular weight materials at different fluid velocities associated with the membrane cartridge.
3. Estimate the model parameters using the method of velocity variation.
4. Investigate the role of solute particle size on the intrinsic rejection coefficient and evaluate the possibility of modeling it as a probability distribution function of the solute molecular weight.

CHAPTER 2

BACKGROUND

2.1 Basic principles of chemistry

In water and wastewater treatment with membrane technology, the environmental engineer encounters systems that contain mixture of two or more molecular species [18]. These mixtures are suspension of small particles including colloidal cells and flocs [16]. The osmotic pressure exerted by these molecular species depends on the type and size of the molecules that comprise the solution. The geometry of these particles is important for defining their different interactions within the fluid system [16].

2.1.1 Particle size and geometry

The performance of many water and wastewater treatment processes is related to the size distribution of organic matter to be treated. Previous research demonstrated that organics can be classified in terms of their size as soluble, colloidal, supracolloidal, and particulate [12, 13] (Figure 1). Several investigators concluded that particle size characterization is of principal importance for more effective design and operation of treatment facilities more effectively [12, 13, 16].

Ultrafiltration is appropriate to separate soluble species that range in molecular size from 500 to 500000 amu [3]. Experience with ultrafiltration indicates that the separation capability of the membranes is influenced by the size and the shape of particles to be separated [2]. Typical organic materials in water and wastewater amenable to UF include recalcitrant compounds, fulvic acids, humic acids, nutrients, chlorophyll, carbohydrates, polysaccharides, proteins, amino acids, vitamins, RNA, fatty acids, and enzymes [10, 12]

(Figure1). Humic and fulvic acids structure have been characterized as flexible linear colloids under natural water pH and ionic strength conditions [10]. It is observed that they change configuration in response to changes in the pH or ionic strength of the solution [10, 16]. Suspension particle geometries of particles vary widely and can include globular, ellipsoids of revolution, thin discs, rods, rod and bead, tree like clusters, or cylinders. Particles may be rigid or flexible random coiled. Polydisperse solutions contain multiple variations of particle size and shape [16].

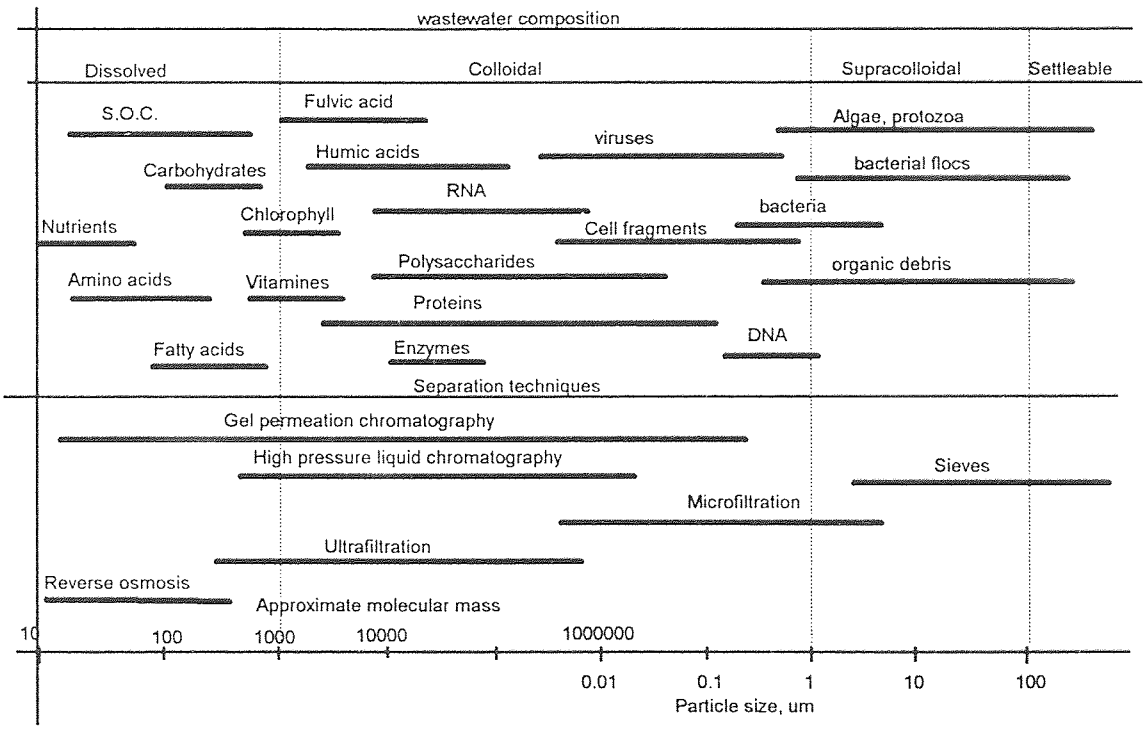

Figure 1. Size range of organic contaminants in wastewater and separation technique for their quantification [13].

Using ultrafiltration a solution can be fractionated into several molecular size classes. Investigation of the molecular geometry specific to each group would reveal the fact that each group is a polydisperse solution but to less extent than that of the original sample [13]. If compounds of similar rejection coefficients are separated, the separation efficiency for each individual species available

depends only on particle geometry. The assumption here is that the rejection coefficient for particles at the same molecular weight are normally distributed around that molecular weight, this molecular weight is an average that encomasses other components in the same class [16].

2.1.2 Osmotic pressure models

The phenomenon of osmotic pressure is illustrated by the apparatus shown in Figure 2. Two solutions that have different solute concentrations are separated by a simipermeable membrane which is impermeable to the solute. The direction of flow is from the more dilute to the more concentrated solution [18]. The water will cross the membrane in both directions, but the net movement will be towards the more concentrated solution [18]. The tendency of solvent to move through simipermeable membranes in the direction of concentrated solutions is termed osmosis [18, 24].

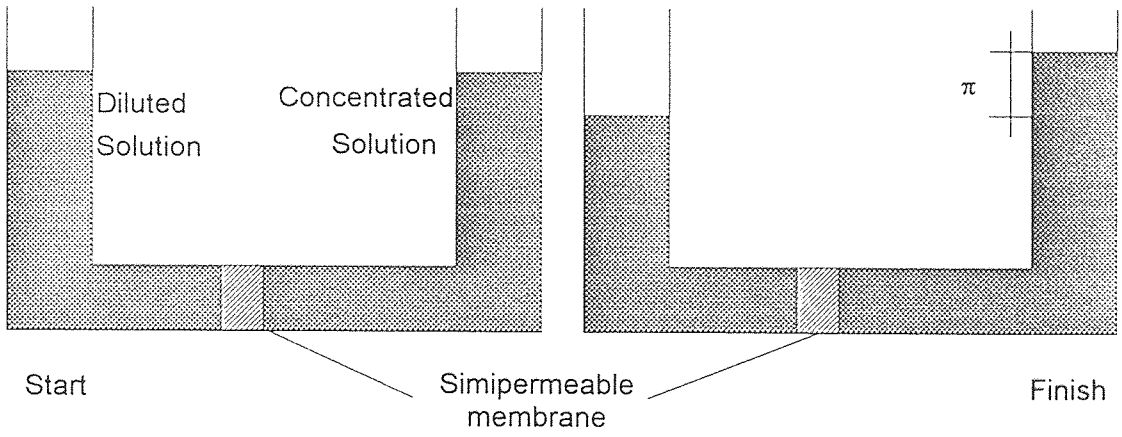

Figure 2. The process of osmosis and the development of osmotic pressure.

A hydrostatic pressure difference will develop between the two compartments as a result of solvent migration. The excess pressure that must be applied to the

solution to produce equilibrium is known as the osmotic pressure and is denoted by the Greek letter π as shown on figure 2. [1]

The net flow of solvent across a membrane is due to a chemical potential difference between the two solutions which can be estimated by the difference in the vapor pressure of the solvent across the membrane [3, 24]. The solvent transfer across the membrane will continue until the effect of hydrostatic pressure overcomes the vapor pressure differential [24]. From this context another definition of osmotic pressure can be derived. Referring to Figure 2 osmotic pressure is the excess hydrostatic pressure that should be applied on the higher concentration side of the cell such that both sides of the cell have the same chemical potential [24].

2.1.2.1 Gibbs model

The osmotic pressure models can be derived from the Gibbs free energy equation, which is written for closed systems in the differential form [23]:

$$dG = VdP - S\,dT \qquad (2.1)$$

where

dG is the free energy change.

V is the volume of the system.

S is the system entropy.

dT is the temperature change of system.

For open systems where matter and energy may enter or leave the system this equation should be modified to account for the free energy changes due to the mass entering or leaving the system [24].

$$dG = VdP - SdT + \sum \mu i\, dNi \qquad (2.2)$$

where

μ is the chemical potential of component i

N is the number of moles of the same component.

Equation 2.2 can be used to define the chemical potential of any component in an open system in terms of the thermodynamic properties of the system. Consider an isothermal and isobaric mass flow out of or into a thermodynamic system of a specific composition, then the chemical potential of that component can be defined as [3, 24]:

$$\mu_i = (\partial G / \partial N_i)_{T,P,Nj} \qquad (2.3)$$

If the temperature and the composition of the system remain constant during the chemical reaction equation 2.2 can be rewritten as [3, 24]:

$$(\partial G / \partial P)_{T,Nj} = V \qquad (2.4)$$

If we take the first derivative of both sides of equation 2.4 with respect to the number of moles of component i, while other components concentrations are not changing in the system., the result is equation 2.5

$$(\partial^2 G / \partial P\ \partial Ni)_{T,Nj} = (\partial V / \partial Ni)_{T,Nj} \qquad (2.5)$$

The right hand side of equation 2.5 represents the partial molar volume of the component of interest, namely $\overline{V}_i$. Equation 2.5 can be rewritten as [3]:

$$(\partial^2 G / \partial P\ \partial Ni)_{T,Nj} = \overline{V}_i \qquad (2.6)$$

If equation 2.3 is differentiated with respect to the pressure and is substituted into equation 2.6 we get [3]:

$$\overline{V}_i = \partial \mu_i / \partial P \qquad (2.7)$$

or

$$d\mu_i = \overline{V}_i dP_i \qquad (2.8)$$

Equation 2.8 has a very important implication, that is the chemical potential of solutions can be changed by changing the external pressure applied to the system[24]. Since the solution is in equilibrium with its vapor pressure the ideal gas law is applicable and when substituted in equation 2.8 it can be rewritten as:

$$d\mu_i = RT\, dP_i / P_i \qquad (2.9)$$

where R is the universal gas constant.

Equation 2.9 indicates that the vapor pressure of a solution is changing in relation to the changes in its chemical potential. Changes in the chemical potential can be induced by changing the mole fractions of either the solvent or the solute. If the chemical potential of the solution is allowed to change to a new value the corresponding change in the vapor pressure can be evaluated by integration of equation 2.9 . The integrated form is [24]:

$$\mu_i^\circ - \mu_{i1} = -RT \ln(P_1 / P^\circ). \qquad (2.10)$$

For ideal solutions the vapor pressure of any component in the solution is directly proportional to the mole fraction of that component in the solution. Written in a mathematical form as[18]:

$$P_1 = X_1 P^\circ \qquad (2.11)$$

where

P_1 is the vapor pressure for any component at the mixture.

X_1 is the mole fraction of that component.

P° is the vapor pressure of that component at its pure state.

Equation 2.11 can be substituted into equation 2.10 and rewritten for the solvent as[24]:

$$\mu_i^\circ - \mu_{i1} = -RT \ln (X_1). \qquad (2.12)$$

When equation 2.8 is integrated, it gives the external pressure that should be applied to equalize the chemical potential of the solution on the two sides of the membrane. For the case where initial condition is the pure solvent, equation 2.8 can be integrated to yield [24]:

$$\mu_i^\circ - \mu_{i1} = \overline{V}_i (P_i^\circ - P^*). \qquad (2.13)$$

Based on the definition of osmotic pressure, it is clear that $(P_i^\circ - P^*)$ is the external pressure which defines the osmotic pressure π. If π is substituted in equation 2.13 instead of $(P_i^\circ - P^*)$, and the appropriate definition for the difference in the chemical potential is substituted from equation 2.12 into equation 2.13 the well known Gibbs law is obtained in the following form[24]:

$$\pi \overline{V}_i = -RT \ln (X_1). \qquad (2.14)$$

2.1.2.2 Van't Hoff model

Van't Hoff developed a mathematical relation for the osmotic pressure that can be derived by approximating the parameters of Gibbs equation. Since X_1 is the mole fraction of the solvent, and X_2 is the mole fraction of the solute then [3]:

$$X_1 + X_2 = 1 \qquad (2.15)$$

$$X_1 = 1 - X_2 \qquad (2.16)$$

In a very dilute solution, X_2 is very small. If we take the logarithm of both sides of equation 2.16. It is possible to rewrite it as:

$$\ln (X_1) = \ln (1 - X_2) \cong -X_2 \qquad (2.17)$$

X_2 is, by definition the mole fraction of the solute that is very small compared to the mole fraction of the solvent. In terms of the number of moles X_2 is written as:

$$X_2 = \frac{N2}{N1+N2} \cong \frac{N2}{N1} \qquad (2.18)$$

where

N_1 is the number of moles of the solvent

N_2 is the number of moles of the solute

Equations 2.17 and 2.18 are substituted into equation 2.14 and written as:

$$\pi \overline{V}_1 = -RT\frac{N2}{N1} \qquad (2.19)$$

or

$$\pi = -RT\frac{N2}{\overline{V1}\,N1} \qquad (2.20)$$

The solvent volume, V is substituted in equation 2.20 in lieu of $\overline{V1}N1$ and rewritten as [3, 24]:

$$\pi = -RT\,\frac{N2}{V} \qquad (2.21)$$

In equation 2.21 $\frac{N2}{V}$ is the molar concentration of the solute (C) and by substituting C in equation 2.21 one gets the Van't Hoff model

$$\pi = -RTC \qquad (2.22)$$

2.1.2.3 Viral coefficients Model

Until now our discussion of osmotic pressure models has been limited to situations where the solution is ideal and homogeneous. In the realm of water and wastewater treatment, the environmental engineer is confronted with heterogeneous solutions that comprise a broad range of molecular sizes. These molecules involve macromolecules, partially hydrolyzed macromolecules, and monomers from different origins. The theoretical treatment of such solutions

stems from the same principles as discussed in the previous sections. To account for the solution heterogeneity, each molecular species is considered to contribute to the total osmotic pressure or,

$$\pi=\sum_{i=1}^{n}\pi_i=\sum_{i=1}^{n}\frac{RTCi}{Mi}=RT\sum_{i=1}^{n}\frac{Ci}{Mi} \qquad (2.23)$$

Equation 2.23 can be rewritten in a more useful form if the left hand side of it is multiplied and divided by the total concentration, C that equals the sum of the individual species concentrations available in solution.

$$\pi=RT\frac{\sum_{i=1}^{n}Ci/Mi\sum_{i=1}^{n}Ci}{\sum_{i=1}^{n}Ci} \qquad (2.24)$$

In equation 2.24 the term $\frac{\sum_{i=1}^{n}Ci/Mi}{\sum_{i=1}^{n}Ci}$ represents the reciprocal of number average molecular weight, $\overline{M_n}$ for the polymers in solution; $\sum_{i=1}^{n}Ci$ represents the solutes concentration. If the notation is introduced into equation 2.24 it can be represented as [24]:

$$\pi=RT\frac{C}{\overline{Mn}} \qquad (2.25)$$

Equation 2.25 constitutes the basics for osmotic pressure evaluation of heterogeneous ideal solutions. However the assumption of ideal solution is valid

only for very dilute solutions, and most real solutions are nonideal over a finite concentration, especially solutions that have large molecules.

Experimental work shows that the non-ideality requires that the osmotic pressure equation include powers of the concentration higher than the first. In many cases, the data can be described by a power series, called the *virial expansion*.[3]

$$\pi = RT\frac{C}{\overline{Mn}} + B_2C_2 + B_3C_3 + \cdots\cdots \qquad (2.26)$$

where

B_2, B_3 are empirical constants termed as the virial coefficients.

2.2 Modeling of membrane separation

There are many uses for mathematical models in engineered systems. In ultrafiltration, models that integrate the physicochemical and hydrodynamic interactions with membranes configuration are used in research to integrate the understanding of the process for hypothesis testing, revealing the relationship between the operation parameters, and to evaluate the experimental results. Models are important in the engineering design of the system to scale up the pilot plant information and to predict the full plant performance under different operating conditions.

The evolution of reactors configurations, and membrane science coupled with the new applications for membranes in treatment facilities and the increased incidence of potential operating problems dictates the necessity for new models, and / or expansion of the existing models.

2.2.1 Transport through membranes

Three distinct theoretical approaches have been used to describe transport in membranes; Kedem-Katchalsky analysis, the solution diffusion model, and the pore model. The first approach was developed directly from the thermodynamic principles of irreversible processes.

In the second approach membranes are treated as nonporous diffusion barriers. All components dissolve in the membrane in accordance with phase equilibrium considerations and diffuse through the membrane by the same mechanisms that control diffusion through solids.

The earliest treatment of the pressure driven membranes were based on a porous model of the membrane. It is assumed in this model that all flow occurs through pores which comprise a certain fraction of the membrane area and which have a characteristic size distribution. Flow rate and solute transfer are governed by the porosity, pore size distribution, solution characteristics, and solute membrane interaction.

2.2.1.1 Kedem-Katchalsky model

2.2.1.1.1 Description

In evaluating membrane transport, the flow of any component is interrelated to the flow of other components. The thermodynamics of irreversible processes provides a useful framework for analysis of dissipative processes.

In this context Kedem and Katchalsky analyzed solute and solvent flux through the membranes and provided a powerful analytical tool for transport analysis of ultrafiltration and reverse osmosis processes. The solvent flux across membranes is assumed to be due to diffusive effects while convective transport is neglected. The volumetric flux is assumed to be directly proportional to the net driving pressure drop across the membrane [9, 10].

$$J_V = L_p (\Delta P - \sigma \Delta \pi) \qquad (2.27)$$

L_p is the coefficient of hydraulic conductivity that depends on the physicochemical properties of the membrane and solution. L_p is directly proportional to the membrane porosity (ε) , the square of the pore radius (a), and liquid density (ρ_l), and inversely proportional to membrane's thickness (δ_m), liquid viscosity (μ), and the square of the pore tortuosity factor (t):

$$L_p = \varepsilon a^2 \rho_l / 8t^2 \mu \delta_m \qquad (2.28)$$

ΔP, $\Delta \pi$ are the net drop in the applied pressure and osmotic pressure respectively; σ is the Staverman reflection coefficient that is a factor between zero and one.

Kedem-Katchalsky analyzed the solute flux ,J_s, as the sum of convective and diffusive transport or [9, 10]:

$$J_S = \omega \Delta \pi + (1 - \sigma') C_f J_V \qquad (2.29)$$

where ω is the local solute permeability, measured at zero volumetric flux. $(1-\sigma')$ is the second solute transport coefficient and can be interpreted as the fraction of solvent flux carried across the membrane by pores large enough to pass solute molecules. If Onsager's reciprocal relations are valid across the membrane, that is, the membrane properties do not change after the application of pressure then $\sigma' = \sigma$, C_f is the feed solute concentration.

2.2.1.1.2 Limitations

While the Kedem-Katchalsky analysis provides a powerful analytical means to evaluate the solute and solvent flux through the membrane, it is not model dependent and sheds no information on solute transfer mechanisms in the liquid

phase. The procedure described by Kedem to evaluate the model parameters is very delicate and very hard to control in the laboratory.

2.2.1.2 Solution diffusion model

2.2.1.2.1 Description

In the solution diffusion model, the membrane is treated as a non porous wall and each component in solution dissolves under high pressure in the membrane in accordance with an equilibrium distribution law and diffuses from the membrane in response to concentration and pressure gradients. Conceptually, the solution diffusion model is useful for describing the reverse osmosis process where essentially highly perm-selective i.e. allows different components in solution to pass in a different degrees. In this analysis, the water flux J_w is proportional to the pressure differential across the membrane that is [6, 20]:

$$J_w = K_w (\Delta P - \Delta \pi) \qquad (2.30)$$

where K_w is the global water mass transfer coefficient that is defined by the following equation [20]:

$$K_w = \frac{D_w \; C'_w \; V_w}{R \; T \; \delta m} \qquad (2.31)$$

where D_w is defined as the water diffusion coefficient through the membrane, C'_w is the water concentration on the membrane surface, V_w is the molar volume of water, R is the universal gas constant, and T is the temperature.

The solute flux is proportional to the difference in solute concentration across the membrane or [6, 20]:

$$J_s = K_s (C_m - C_p) \qquad (2.32)$$

where K_s is the solute flux through the membrane, is the mass transfer coefficient of the solute that is [20]:

$$K_s = \frac{D_s . K_d}{\delta_m} \qquad (2.33)$$

where D_S is the solute diffusion coefficient through the membrane, K_d is the distribution coefficient for the solute. C_m is the solute concentration on feed side of the membrane, C_p is the permeate solute concentration.

2.2.1.2.2 Limitations

In applications of the solution diffusion model, both the solvent flux and solute flux are functions of the solute concentration on the membrane surface. However it does not provide with any information to evaluate this concentration. It does not consider the effect of transport of any component on the transport of the other component i. e. flow coupling. Modeling the membrane as nonporous media can not adequately describe ultrafiltration membranes that are characterized by high porosity. Dissolution of high molecular weight materials in the membrane phase is not addressed.

2.2.1.3 Pore model

2.2.1.3.1 Description

Physically, separation occurs either because solutes are too large to enter the pores or, because of frictional interaction between the solute and pore walls. In this simplified view of membranes, pores are treated as very fine capillary tubes of uniform radius piercing the membrane body at right angles. The rate at which a fluid flows through a tube depends on the tube dimensions, fluid viscosity of the fluid, and the pressure drop between the ends of the tube. Based on this concept, the water flux through the membrane is given in terms of pore radius by Poiseuille's equation in the form [24]:

$$J_W = \frac{\varepsilon a^2 \Delta P}{8 \mu \delta_m} \qquad (2.34)$$

2.2.1.3.2 Limitations

This relationship is too simple to adequately describe real membrane operations for several reasons. Pore tortuosity, blind pores, and dispersion in the pores radii are all neglected. In addition, this model gives no information about solute flux across the membrane or hydrodynamic effects on solvent or solute flux. In situations of high concentration, the membrane and associated boundary layer resistance are continuously changing.

2.2.2 Transport through ultrafiltration cells

Large scale membranes for environmental engineering applications typically comprise a tangential flow configuration in which the bulk flow of water travels in a direction parallel to the membrane surface. As illustrated in figure 3, the solute is convectively transported to the membrane as a result of the fluid permeation across the membrane.

Some fraction of the solute can diffuse through the membrane with the solvent, while another fraction is retained. The continuous fractionation of solute on the membrane surface results in a higher concentration on the membrane surface than that of the bulk fluid. The solute is then transported back to the solution by Brownian diffusion. When steady state prevails in the flow channel, the convective transport is counterbalanced by the sum of diffusive transport and solute fraction that permeate the membrane

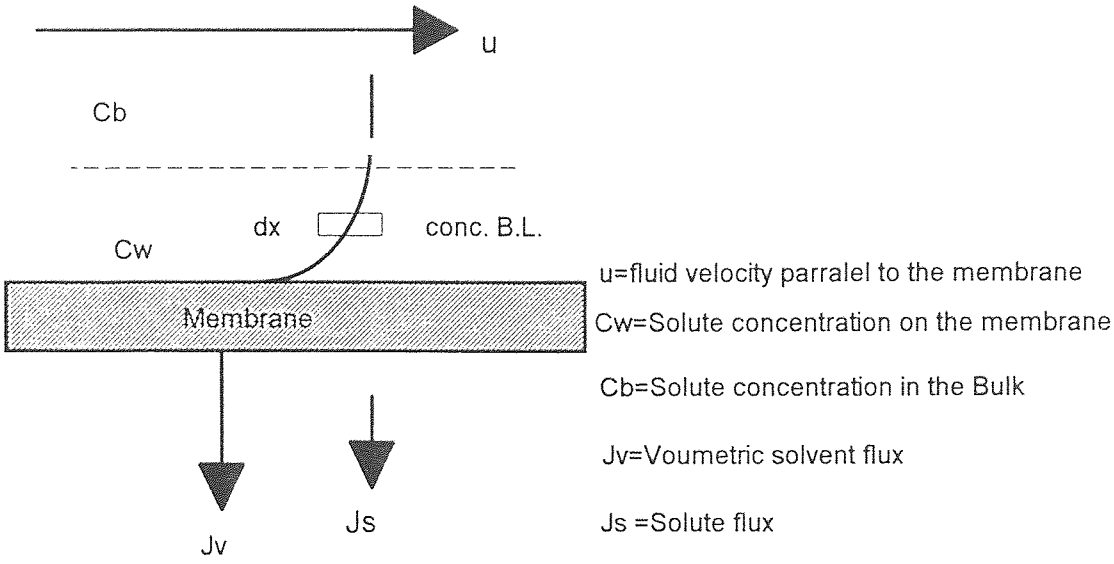

Figure 3. Elements of tangential flow system.

This is mathematically expressed on a differential element on the concentration boundary layer as [17]:

$$J_V C = J_V C_p + D \frac{dc}{dx} \qquad (2.35)$$

If the variables are separated equation 2.35 it can be expressed in the following form [17]:

$$\frac{J_v}{D} dx = \frac{dc}{C - C_p} \qquad (2.36)$$

Equation 2.36 can be integrated over the concentration boundary layer and substitution of the following boundary conditions [17]:

$$C = C_w \text{ at } X = \delta \qquad (2.37)$$

$$C_b \text{ at } X = 0 \qquad (2.38)$$

$$\frac{\delta J_v}{D} = \text{Ln} \frac{C_w - C_p}{C_b - C_p} \qquad (2.39)$$

where:

D = Solute diffusion coefficient.

δ = Concentration boundary layer thickness.

C_w, C_b, C_p are solute concentration on the wall, bulk,

and permeate respectively.

Equation 2.39 can be rewritten if the appropriate term for $\frac{D}{\delta}$ is substituted as K, the coefficient for mass transfer and arrangement in the following form:

$$\frac{C_w - C_p}{C_b - C_p} = \text{Exp}\frac{J_v}{K} \qquad (2.40)$$

CHAPTER 3

MODEL DEVELOPMENT

3.1 Basic principles

The probability that a component will permeate a membrane is defined as the ratio of solute concentration in the permeate, C_p, to the solute concentration on the surface of the membrane, C_w, and is defined as

$$P = \frac{C_p}{C_w} \qquad (3.1)$$

Equation 3.1 defines the permeation coefficient, and it's complement defines the fractional reduction in the feed concentration across the membrane (the intrinsic rejection factor) , σ_i, or

$$\sigma_i = 1 - P = 1 - \frac{C_p}{C_w} \qquad (3.2)$$

Equation 3.2 can be rearranged and solved for the permeate concentration in terms of the solute concentration at the wall and the intrinsic rejection factor as

$$C_p = (1 - \sigma_i) C_w. \qquad (3.3)$$

Equation 3.3 can also be developed from Kedem-Katchalsky's model for solute fluxes. Recalls equations 2.27 and 2.29 and changing the notation for the feed concentration to be the concentration on the membrane surface [9].

$$J_V = L_p(\Delta P - \sigma \Delta \pi) \qquad (2.27)$$

$$J_S = \omega \Delta \pi + (1 - \sigma') C_W \ J_V. \qquad (2.29)$$

In the application of equations 2.27 and 2.29 to systems characterized by moderate concentrations of high molecular weight solutes, the osmotic pressure is small and can be neglected [10]. If this approximation is introduced into equations 2.27 and 2.29 they can be modified as [9]:

$$J_V = L_p \Delta P \qquad (3.4)$$

$$J_S = (1 - \sigma_i) C_w J_V. \qquad (3.5)$$

The solute concentration is defined as the ratio of the solute flux to the solvent flux or [9, 10]

$$C_p = \frac{Js}{Jv} \qquad (3.6)$$

Equations 3.4, 3.5, and 3.6 when combined together yield an expression for the solute rejection coefficient.

$$\frac{Cp}{Cw} = \frac{Js}{Cw Jv} = \frac{(1-\sigma i) Cw\ Jv}{Cw\ Jv} = 1-\sigma i \qquad (3.7)$$

If the left hand side of equation 3.7 is cross multiplied by the right hand term of the same equation we get an expression for the solute concentration in the permeate the same as was obtained in equation 3.3 as

$$C_p = (1 - \sigma_i) C_w. \qquad (3.3)$$

The stagnant film theory provides an analytical tool to evaluate the concentration of solute at the membrane surface. Recall equation 2.40

$$\frac{C_w - C_p}{C_b - C_p} = \mathrm{Exp}\frac{J_v}{K} \qquad (2.40)$$

An expression for the solute concentration at the membrane surface can be derived from equation 2.40 if it is cross multiplied and rearranged.

$$C_w = C_p + (C_b - C_p) \exp\frac{Jv}{K} \qquad (3.8)$$

Before equation 3.8 can be substituted into equation 3.3 we must obtain an appropriate expression for the coefficient of mass transfer, K, and solve for the mean solute concentration on the bulk fluid stream, C_b.

3.2 Mass transfer coefficient estimation

There are several theoretical and experimental developments that have been reported to evaluate the coefficient of mass transfer [3]. The experimental data for mass transfer coefficients obtained for various kinds of solutions and different cell geometries can be correlated using dimensionless numbers. The most important dimensionless number is the Reynolds number N_{Re}, which represents the ratio between the inertial and viscous forces [6].

$$N_{Re} = \frac{d_h u \rho}{\mu} \qquad (3.9)$$

where d_h is the hydraulic radius of the flow channel, u the mean stream speed past the membrane, ρ is the fluid density, and μ is the viscosity.

The Schmidt number, N_{Sc} is [6]

$$N_{Sc} = \frac{\mu}{\rho D} \qquad (3.10)$$

where D is diffusion coefficient. The Schmidt number is the ratio of the shear component for diffusivity μ / ρ to the diffusivity for mass transfer D, and it physically relates the relative thickness of the hydrodynamic layer and mass transfer boundary layer.

The Sherwood number N_{Sh}, which is dimensionless, is [6]

$$N_{Sh} = \frac{Kdh}{D} \qquad (3.11)$$

where K is the coefficient of mass transfer. In the molecular transport of momentum, heat, or mass there are many similarities. The molecular diffusion equations of Newton for momentum, Fourier for heat, and Ficks for mass are

very similar and can be used to develop an analogy among these three molecular transport processes.

A great deal of effort has been devoted in the literature to develop analogies among these three transport processes. The most successful and most widely used analogy is the Chilton and Colburn J -factor analogy. This analogy is based on experimental data in both laminar and turbulent flow regimes and is written as follows [1, 4]:

$$J_D = \frac{K}{u} N_{Sc}^{2/3} = f/2 \qquad (3.12)$$

where f is the flow friction factor.

Equation 3.12 is useful in correlating the momentum and mass transfer, and permits the prediction of the unknown mass transfer in terms of the friction factor. In turbulent flow the friction factor is directly proportional to the Reynolds number and can be correlated using the Blasius formula as [1]:

$$f = 0.0791\ N_{Re}^{(-0.25)} \qquad (3.13)$$

If equation 3.13 is substituted into equation 3.12 we get the expression for the coefficient of mass transfer as [1, 6]:

$$\frac{K}{u} N_{Sc}^{2/3} = 0.04\ N_{Re}^{(-0.25)} \qquad (3.14)$$

or

$$\frac{K}{u} = 0.04\ N_{Re}^{-0.25}\ N_{Sc}^{-2/3} \qquad (3.15)$$

It has been shown that for convective mass transport the dimensionless numbers are correlated and yield the following form [6]

$$N_{Sh} = f[\ N_{Re}\ ,\ N_{Sc}] \qquad (3.16)$$

If equation 3.15 is multiplied by $\frac{dh}{D}$ and u is cross multiplied the resulting form can be grouped in the form of equation 3.16 or

$$N_{Sh} = 0.04\, N_{Re}^{0.75}\, N_{Sc}^{1/3} \qquad (3.17)$$

It has been shown that equation 3.17 tends to fit the experimental data more closely if the right hand term is modified as [8]

$$N_{Sh} = 0.023\, N_{Re}^{0.9}\, N_{Sc}^{1/3} \qquad (3.18)$$

Equation 3.18 has been validated by experimental results for turbulent flow. In equation 3.18 the only variable parameters are the mass transfer coefficient and the mean fluid velocity past the membrane. The mass transfer coefficient can be evaluated in relation to the mean fluid velocity as

$$K=0.023\frac{D^{0.667}\times\rho^{0.567}}{(d_h)^{0.1}\times\mu^{0.567}}\,u^{0.9} \qquad (3.19)$$

3.3 Mean local solute concentration evaluation

The solute concentration in the bulk solution or the mean local brine concentration can be estimated using flow weighted average values between the inflow and the retentate concentrations, or [23]:

$$C_b=\frac{Q_iC_i+Q_rC_r}{Q_i+Q_r} \qquad (3.20)$$

Referring to Figure 4 one may write material mass balance relationships for both the solvent and solute that for the solute mass balance is:

$$Q_i\, C_i = Q_p\, C_p + Q_r\, C_r \qquad (3.21)$$

And, the solvent mass balance relationship is:

$$Q_i = Q_p + Q_r \qquad (3.22)$$

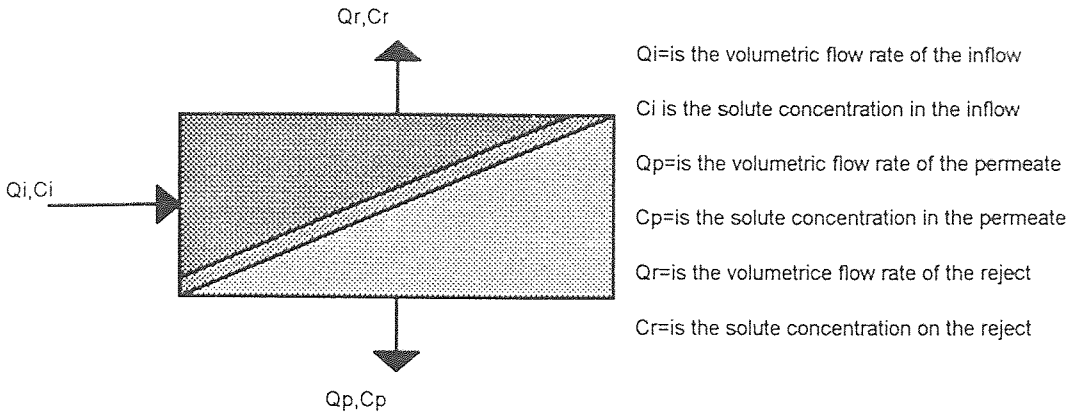

Figure 4. Definition of inflow and outflow parameters associated with ultrafiltration cell.

Q_r can be written in terms of the inflow and permeate flow by arrangement of equation 3.22 as

$$Q_r = Q_i - Q_p \qquad (3.23)$$

Equation 3.23 is substituted in equation 3.21 to solve for the solute concentration on the retentate as

$$Cr = \frac{Q_i C_i - Q_p C_p}{Q_i - Q_p} \qquad (3.24)$$

When equations 3.23, and 3.24 are substituted in equation 3.20 an expression is obtained that correlates the mean solute concentration in the bulk fluid in terms of the feed concentration and permeate concentration as

$$Cb = \frac{2Q_i C_i - Q_p C_p}{2Q_i - Q_p} \qquad (3.25)$$

Equations 3.25, and 3.19 are substituted into equation 3.8 and grouping the concentration terms on the left hand side one gets

$$\frac{C_p}{C_i - C_p} = \frac{1-\sigma_i}{\sigma_i}\frac{2Q_i}{2Q_i - Q_p}\,Exp\frac{J_v}{0.023\dfrac{D^{0.667}\times\rho^{0.567}}{(d_h)^{0.1}\times\mu^{0.567}}u^{0.9}} \qquad (3.26)$$

Introducing the filtration efficiency concept into equation 3.26 that is defined as the percentage reduction in the solute concentration from the feed, or:

$$E = \frac{C_i - C_p}{C_i} \qquad (3.27)$$

The relation for the solute removal efficiency is written as

$$\frac{1-E}{E} = \frac{1-\sigma_i}{\sigma_i}\frac{2Q_i}{2Q_i - Q_p}\,Exp\frac{J_v}{0.023\dfrac{D^{0.667}\times\rho^{0.567}}{(d_h)^{0.1}\times\mu^{0.567}}u^{0.9}} \qquad (3.28)$$

If we assume that the solvent flux across the membrane is uniform, Q_i can be rewritten in terms of the permeate flow, Q_p, and the mean flow along the feed channel, Q_m.

$$Qi = Qm + \frac{Qp}{2} \qquad (3.29)$$

If equation 3.29 is substituted in the term $\frac{2Q_i}{2Q_i - Q_p}$ of equation 3.28 it can be expressed in terms of the new parameters as:

$$\frac{2Qm + Qp}{2Qm} = 1 + \frac{Qp}{2Qm} \qquad (3.30)$$

But Q_p equals J_V multiplied by the permeation area of the membrane, A_m, and Q_m equals the average fluid velocity past the membrane multiplied by the cross section of the flow channel, A_c. By substitution in equation 3.30 one gets

$$\frac{2Qm + Qp}{2Qm} = 1 + \frac{Jv\,Am}{2u\,Ac} \qquad (3.31)$$

This expression is then substituted into equation 3.28 to yield

$$\frac{1-E}{E}=\frac{1-\sigma_i}{\sigma_i}\left(1+\frac{J_v A_m}{2uA_c}\right)\mathrm{Exp}\frac{J_v}{0.023\dfrac{D^{0.667}\times\rho^{0.567}}{(d_h)^{0.1}\times\mu^{0.567}}u^{0.9}} \quad (3.32)$$

If we take the natural logarithm of both sides of equation 3.32 and rearrangement the terms one gets

$$\ln\frac{1-E}{E}-\ln\frac{1-\sigma_i}{\sigma_i}=\frac{Jv}{0.023\dfrac{D^{0.667}\times\rho^{0.567}}{(d_h)^{0.1}\times\mu^{0.567}}u^{0.9}}+\ln\left(1+\frac{J_v A_m}{2uA_c}\right)$$

(3.33)

If $\frac{JvAm}{2uAc}$ is designated as X, then the term in the bracket in equation 3.33 can be written as ln (1+X). In turbulent flow the volumetric flux is much less than the fluid speed past the membrane, hence X is much less than 1 and ln (1+X) can be expanded in a power series as

$$\ln(X+1)=\sum_{n=1}^{\infty}\frac{(-1)^{n-1}X^n}{n} \quad (3.34)$$

In equation 3.34 the exponents higher than 1 can be neglected and ln (1+X) can be approximated by X. By substituting of the appropriate terms in equation 3.33 one gets

$$\ln\frac{1-E}{E}-\ln\frac{1-\sigma_i}{\sigma_i}=\frac{Jv}{0.023\dfrac{D^{0.667}\times\rho^{0.567}}{(d_h)^{0.1}\times\mu^{0.567}}u^{0.9}}+\frac{J_v A_m}{2uA_c}$$

(3.35)

If the exponent of velocity in the second term of the right hand term of equation 3.35 is changed to 0.9 instead of one the equation can be rewritten as:

$$\ln\frac{1-E}{E}-\ln\frac{1-\sigma_i}{\sigma_i}=\frac{J_v}{u^{0.9}}\left\{\frac{1}{0.023\dfrac{D^{0.667}\times\rho^{0.567}}{(d_h)^{0.1}\times\mu^{0.567}}}+\frac{u^{0.1}A_m}{2A_c}\right\}$$

(3.36)

Experimental results show that the velocity term $u^{0.1}$ in equation 3.36 varies in a very small range that make it possible to approximate ($u^{0.1}$ /2) by a constant, K'. The exact value of K' depends on the velocity measurement units and flow regime in the membrane cartridge (From the experimental work done in this thesis K'=0.75 is good approximation for the units used). Introduction of this constant in equation 3.36 one can rewrite it as:

$$\ln\frac{1-E}{E}=\ln\frac{1-\sigma_i}{\sigma_i}+\left\{\frac{(d_h)^{0.1}\times\mu^{0.567}}{0.023D^{0.667}\times\rho^{0.567}}+\frac{K'A_m}{A_c}\right\}\frac{J_v}{u^{0.9}}$$

(3.37)

Investigation of equation 3.37 has the following features:

1. Equation 3.37 is a linear equation that has the form.

$$Y = m + sX$$

where, m is the intercept that equal $\ln\frac{1-\sigma_i}{\sigma_i}$, s is the slope that equals $\left\{\frac{(d_h)^{0.1}\times\mu^{0.567}}{0.023D^{0.667}\times\rho^{0.567}}+\frac{K'A_m}{A_c}\right\}$, Y is $\ln\frac{1-E}{E}$, and X equals $\frac{J_v}{u^{0.9}}$. A plot of $\ln\frac{1-E}{E}$ versus $\frac{J_v}{u^{0.9}}$ on the abscissa of linear coordinates one gets a straight line that can be extrapolated to the intercept of $\ln\frac{1-\sigma_i}{\sigma_i}$ from which we can evaluate the intrinsic rejection coefficient for the solute.

2. The membrane characteristics and flow hydrodynamics can be used to measure the removal efficiency in ultrafiltration.
3. An alternative definition for the intrinsic rejection coefficient is the maximum solute removal efficiency that can be attained at solution velocities equal to infinity in the membrane cartridge previously defined as the solute rejection efficiency at zero volumetric flux.
4. This model evaluates the efficiency based on fixed parameters i.e. the intrinsic rejection coefficient, diffusion coefficient, and viscosity and variable parameters i.e. fluid velocity, volume flux, and cartridge dimensions. A major advantage of this approach is that role of each parameter on the pilot plant results is carified and can be readily extrapolated to full scale plant design.

CHAPTER 4

EXPERIMENTAL DESIGN

In this research the rejection capability of an ultrafiltration was examined by the application of solution that have different molecular weight solutes. The solutions were examined by the method of velocity variation where the operating pressure and the bulk concentration were kept constant during the whole experimental runs. Once the steady state was achieved flow was measured and samples from the permeate, retentate and inflow were taken for concentration analysis. The pumping speed was changed to alter the solution velocity in the membrane cartridge. In this approach we allow the permeate concentration to be change as a result of the solution velocity not by other parameters i.e. pressure, feed concentration.....etc.

Details about solutes and materials, samples preparation, apparatus, flow diagram, and laboratory methodology and analysis are presented in this section of this thesis. More specific details about samples preparation and laboratory methodology is located in appendix A of this thesis.

4.1 Solutes and materials

The solutes used in this research were Polyethylene Glycol (PEG), Solid polymers of the general formula H (O CH2-CH2)$_n$.OH, or where n is greater than or equal 4 (Fluka Chemical Corp., Ronkonkoma, NY.). It's structural formula is illustrated in Figure 5. In general each PEG is followed by a number which corresponds to its average molecular weight.

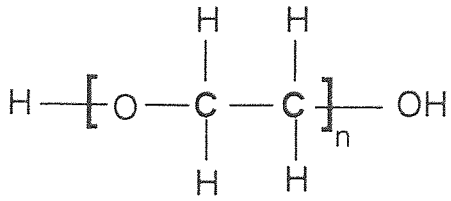

Figure 5. The general structural formula of PEG.

PEG was purchased as a clear white solid which dissolves in water. Glycols do not hydrolyze or deteriorate on storage. Polyethylene Glycols are compounds of low toxicity.

4.2 Samples preparation

Solutions of different molecular weight (PEG 2000, PEG 4000, PEG 8000, PEG 12000) were prepared at 0.05% concentration in a saline solution using Sodium Chloride reagent such that all the experiments were run under constant ionic strength of 0.005. Solutions of PEG 6000, and PEG 10000 were prepared by mixing the appropriate volumes of PEG 4000, and PEG 8000 or PEG12000 and PEG 8000 respectively. A 10^{-3}M phosphate buffer solution is used to control the feed solutions pH to 7.0 ± 0.2.

4.3 Apparatus

The ultrafiltration system used in this study was CH2PR Model hollow fiber concentrator (Amicon, Inc., Beverly, MA, USA). It consists of 2 liter reservoir, CH2 hollow fiber adapter, variable speed peristaltic pump, back-pressure valve, pressure gage, high speed switch, and tubing. The membrane used in this study was an advanced hydrophilic polysulfone hollow fiber (H1P10-43) 10000 nominal molecular weight cut-off. Each cartridge consists of 55 fibers that have 1.1 mm inside diameter and 0.03 m^2 total surface area (manufacturer catalog).

4.4 Flow diagram

The pilot scale UF system used in this study consisted of a hollow fiber membrane cartridge equipped with a two liter feed tank which was connected to a peristaltic pump that has the capability to pressurize the feed solution at variable velocity (Figure 6). The velocity of the feed through the membrane cartridge is controlled by the velocity switch that has ten different readings ranging from zero to ten. A five liter holding tank was added to the system to increase the volume of the feed that can be processed on a continuous mode of operation. The pressure drop across the membrane was measured by two pressure gages installed on the feed and retentate lines.

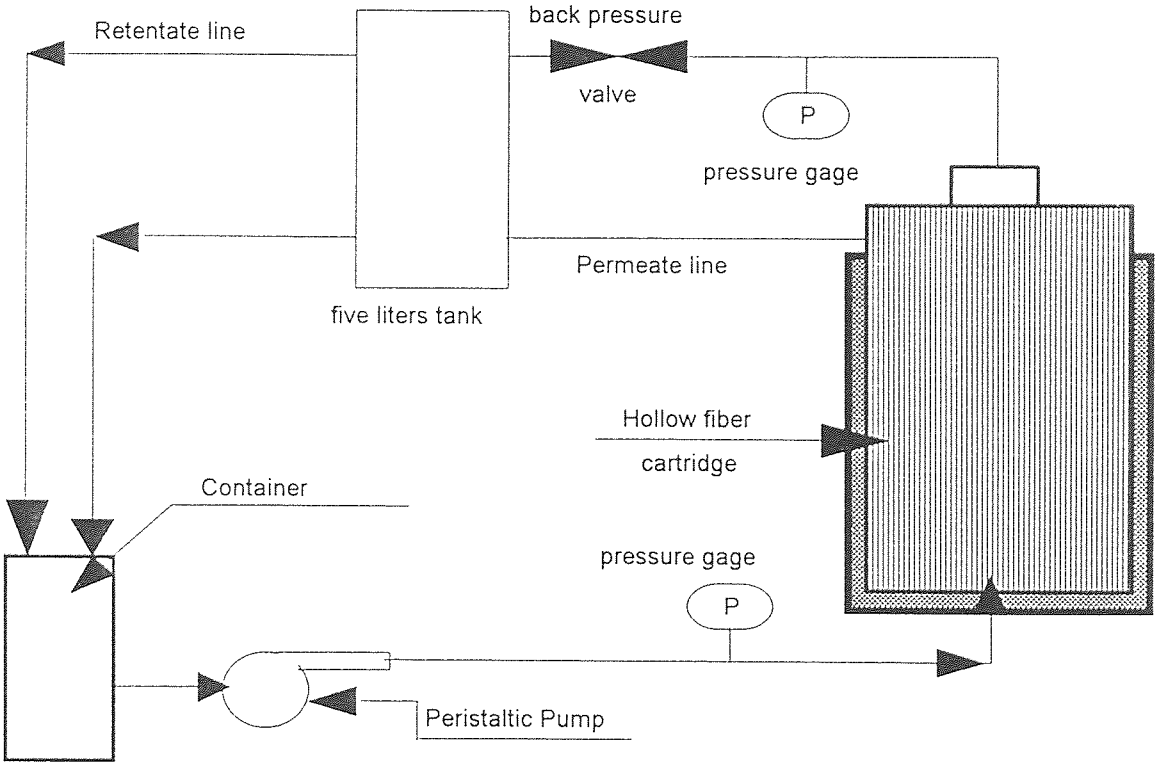

Figure 6. Flow diagram and apparatus set up for all ultrafiltration experiments.

The permeate exits from the cartridge at one atmosphere. A back pressure valve is installed on the retentate line to readjust the pressure when it is desirable to

change the flow velocity while operating at constant pressure. Both the permeate and the retentate were collected in the five liter tank for mixing and recycling. The volumetric flow is measured by collecting 500 milliliters of the solution in a graduated cylinder and measuring the corresponding time by a stop watch.

4.5 Laboratory methodology and analysis

All prepared solutions were examined by the method of velocity variation. The operating pressure and the solute concentration in the bulk fluid were kept constant for each individual solution. The initial filtration process was conducted at 20 psi and the maximum pumping speed. Samples were extracted for concentration and flow measurements after steady state was attained. The pumping speed was controlled such that the fluid velocity in the membrane cartridge is changed to the desired level. The pressure is changed by the back pressure valve such that all the experiment are run at the same initial pressure.

The concentration data was used to evaluate the solute rejection efficiency using equation 3.27 and the flow data were directly used to measure the volumetric flux and the solution velocity in the cartridge.

CHAPTER 5

RESULTS AND DISCUSSION

5.1. The coefficient of hydraulic conductivity

The coefficient of hydraulic conductivity for pure (MQ) water was determined for the used membrane from the slope of a corresponding plot of volumetric flux, J_v as a function of the transmembrane pressure drop as illustrated in Figure 7.

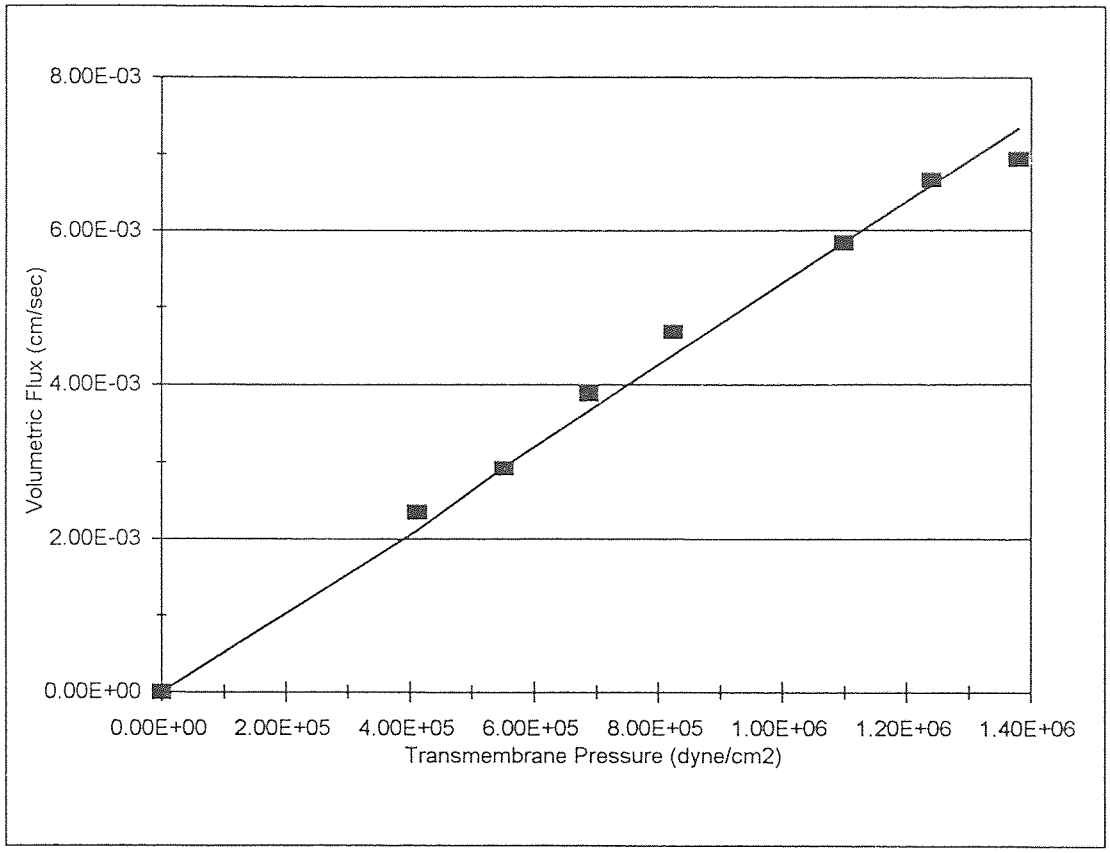

Figure 7. The relationship between the volumetric flux and transmembrane pressure for (MQ) water.

A linear relationship between flux and the pressure was found for the 10K membrane used in the experimental work over the pressure margin recommended by the manufacturer. The coefficient of hydraulic conductivity can

estimated from Figure 7 for the 10 K membrane and is 5.32E-9 $cm^3.dyne^{-1}.sec^{-1}$. The coefficient of hydraulic conductivity is a parameter that depends only on the membrane characteristics and the fluid kinematic viscosity and can be evaluated for other solutions using the following equation:

$$\frac{L_{p1}}{L_{p2}} = \frac{\nu_2}{\nu_1} \qquad 5.1$$

where L_{p1} is the coefficient of hydraulic conductivity of pure (MQ) water, L_{p2} is the coefficient of hydraulic conductivity for the solution, ν_1 and ν_2 are the kinematic viscosity of the (MQ) water and solution respectively.

The linear relation between volumetric flux and transmembrane pressure also indicates that the membrane conforms to the volumetric flux relation of Kedem-Katchalsky's model (equation 2.27 in this text).

5.2. Efficiency and solution mean velocity in the membrane cartridge

The steady state removal efficiency for Polyethylene glycol solutions were evaluated at different solution velocities as shown in Table 1.

Table 1. Removal efficiency for different solutions at different solution velocity.

PEG4000		PEG6000		PEG8000		PEG10000		PEG12000	
u cm/s	E %	u cm/s	E %	u cm/s	E %	u cm/s	E %	u cm/s	E %
71.4	10	80.9	12.8	79.8	15.4	79.7	16.9	77.6	16
64.9	7.6	72.9	9.9	73.5	7.7	74.9	12	71	13.5
57.4	4.4	60.8	6.1	63.1	5.3	63.5	9.9	64.3	10.8
42.7	2.5	44.5	2.3	56.8	3.8	48.2	3.5	48	4.3
33.2	1.3	34	1.5	40.8	2.6	35.7	1.8	36.5	2

Examination of Table 1 shows that the removal efficiency increases with increasing solution velocity in the membrane cartridge. This drastic change occurs with only two fold margin of velocity change. These results emphasize the need for consideration of velocity and concentration polarization as principal parameters in the treatment efficiency evaluation of water and wastewater treated by ultrafiltration membranes.

5.3 Evaluation of the model parameters

The effects of flow hydrodynamics on the removal efficiency are investigated using the mathematical model developed in chapter 3 of this document. Plots of J_v / $u^{0.9}$ versus $\ln\frac{1-E}{E}$ obtained from the experimental results for different molecular weight PEG solutions are shown in Figures 8, 9, 10, 11, and 12.

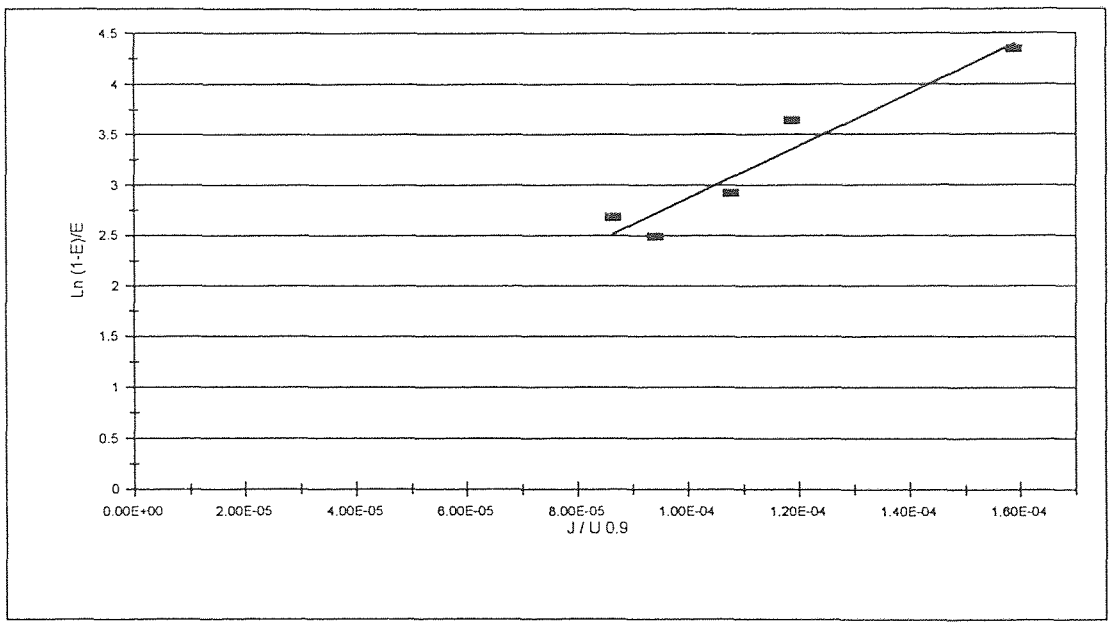

Figure 8. Velocity effects on the rejection efficiency of PEG 4000 solution.

A close fit was obtained for all solutions used, represented by coefficient of correlation R^2 range from 85.9% to 98.9%. If the regression line is extended to

cross the Y-axis the intercept represents the efficiency at zero volumetric flux or infinite velocity, this intercept represent $\ln\frac{1-\sigma_1}{\sigma_1}$ from which the intrinsic rejection coefficient can be evaluated. The model parameters are evaluated from the plots (Figs. 8-12) relevant to each molecular weight are given in Table B.2.

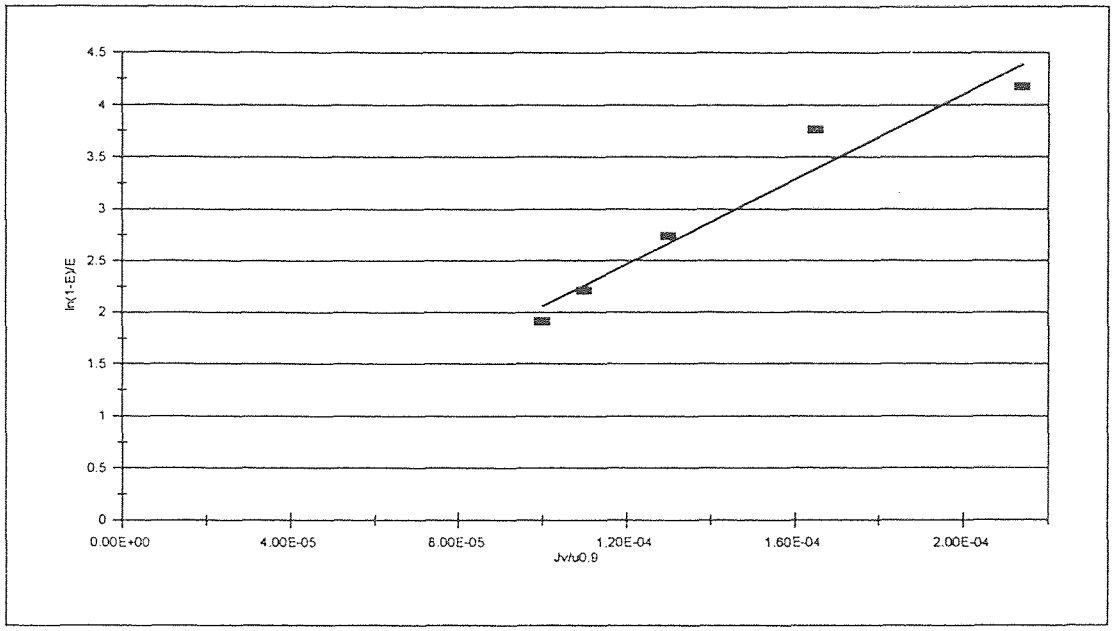

Figure 9. Velocity effects on the rejection efficiency of PEG 6000 solution.

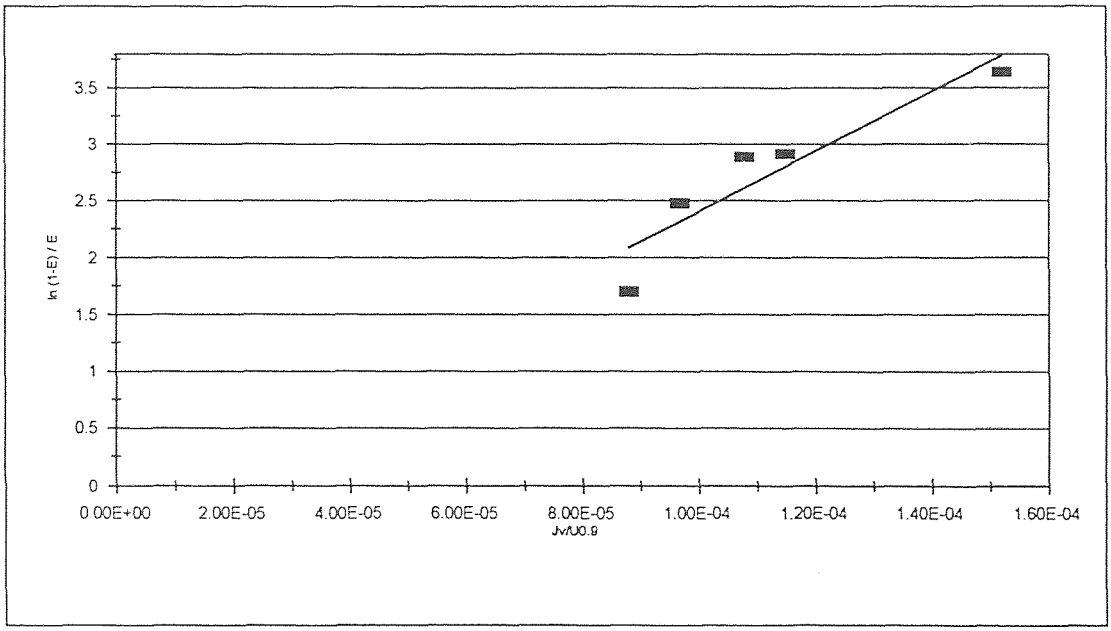

Figure 10. Velocity effects on the rejection efficiency of PEG 8000 solution.

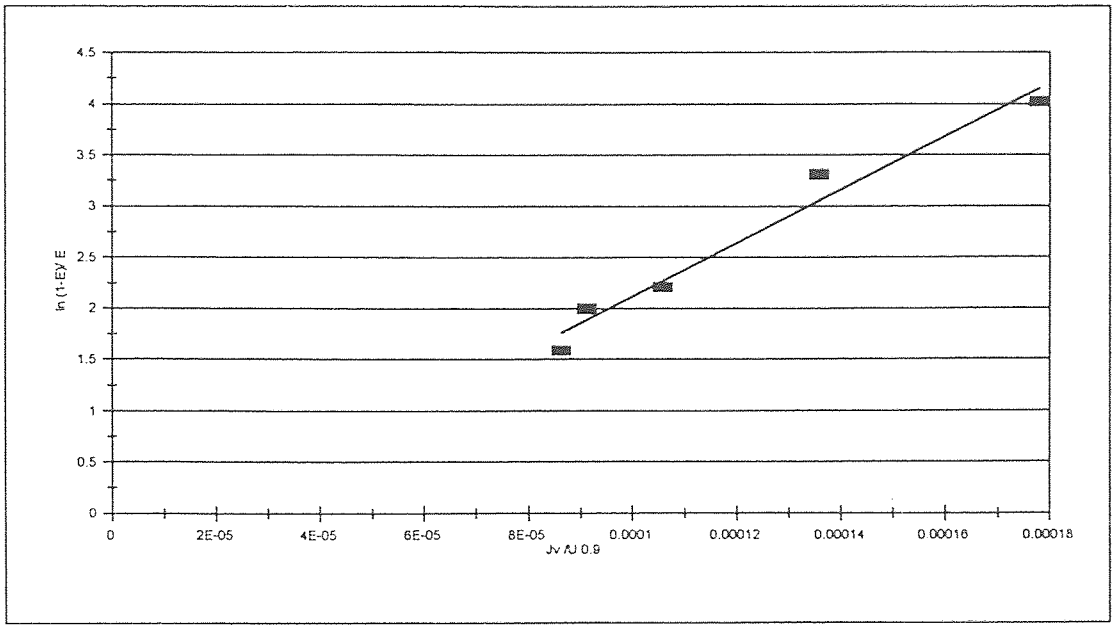

Figure 11. Velocity effects on the rejection efficiency of PEG 10000 solution.

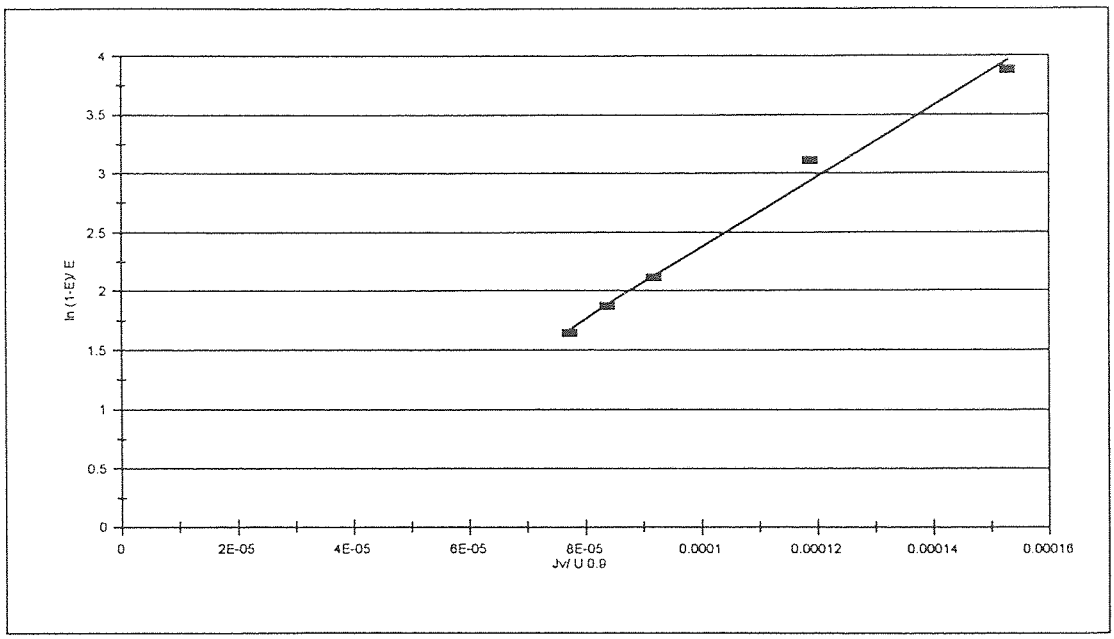

Figure 12. Velocity effects on the rejection efficiency of PEG 12000 solution.

According to equation 3.37 the slope of the linearized model is function only of the fluid parameters (μ, ρ, and D) and the cartridge dimensions (A_c, A_m, d_h).

This implies that the slope of the linear relationship should show a trend as the solution molecular weight changes. The trend either increases or decreases depending on the relative influence of viscosity or diffusion coefficient. Based on the results reported in Table B.2 of the Appendix the slope don't have such a trend we believe the reason for that is the discrepancy may be due to the concentration of the solutions used in fractionation test may have occured, or pressure change during the testing. In any case these effects should not have impact on the intrinsic rejection coefficient since its neither concentration nor pressure dependent.

The intrinsic rejection coefficient computed from the linear plots (Figures 8-12) is used to estimate the solute concentration on the membrane internal face at different solution velocities and is given in Table B. 3 of the appendix. It is shown (Table B.2) that the ratio of solute concentration on the wall to inflow solute concentration ranges between 1.58 and 2.86 for the solutions used and prevailing experimental conditions. This ratio increases as the fluid velocity decreases for the same solute and increases as the solute molecular weight increase. These results emphasize on the need for models that take into account the concentration on the membrane surface rather than on the feed channel.

5.4 Rejection coefficient as a function of molecular weight

The intrinsic solute rejection coefficients for solutions with different molecular weights are plotted on a log-log scale as a function of the molecular weights on Figure 13. The intrinsic rejection coefficient expectedly increases with the solute molecular weight supporting the consideration of ultrafiltration as a size exclusion process. Figure 13 also shows that the rejection coefficient tend to fit a straight line on a log-log plot over the available range of molecular weights. This tendency in the rejection coefficient data remarks the possibility of simulating the

intrinsic rejection coefficient as a log-normal probability distribution function of the solute molecular weight.

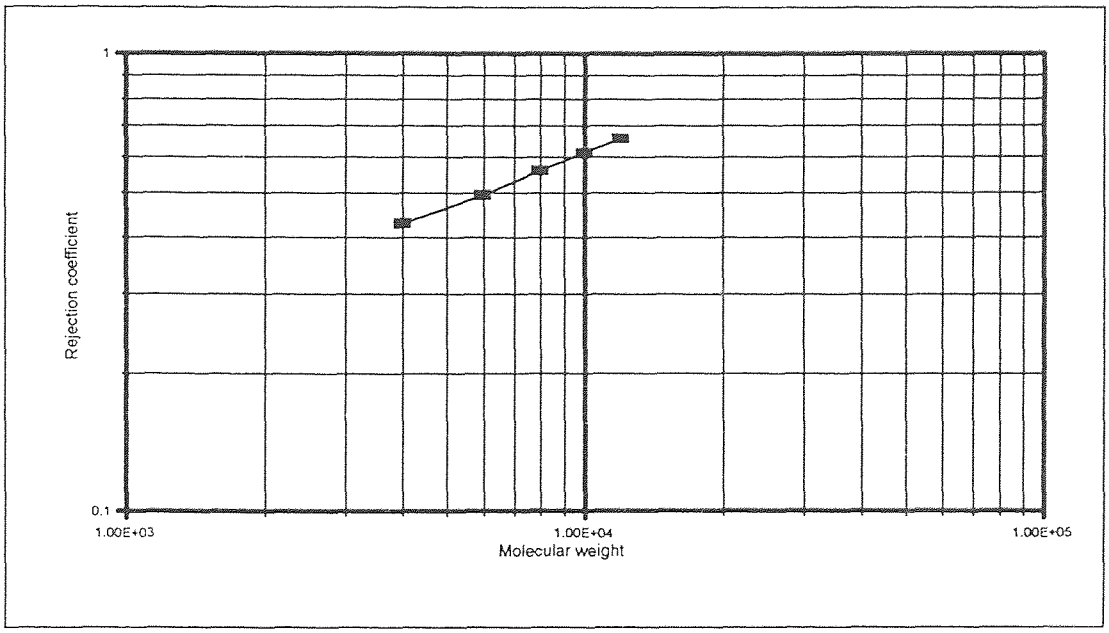

Figure 13. Relationship between the molecular weight and the rejection coefficient.

Further experimental work is required to evaluate the intrinsic rejection coefficient for higher molecular weight solutes on the same membrane and other membranes.

CHAPTER 6

CONCLUSIONS

1. The solute rejection efficiency decreases in responce to decreases in the flow velocity in the membrane cartridge and vise versa.
2. The experimental data fits the proposed mathematical model very closely suggesting its suitability to evaluate the rejection efficiency in ultrafiltration.
3. The mathematical model can be used to evaluate the intrinsic rejection coefficient that can be used to determine the solvent flux in Kedem - Katchalisky model.
4. The intrinsic rejection increases as a function of the molecular weight of the solute supporting the consideration of ultrafiltration as sieving.
5. The plot of the intrinsic rejection coefficient indicate that modeling the intrinsic rejection coefficient as log-normal probability distribution function is realistic.

APPENDIX A

LABORATORY METHODOLOGY AND ANALYSIS

A.1 The coefficient of hydraulic conductivity

Pure (MQ) water was pumped in each membrane until all glycerin that covers the membrane was removed. The coefficients of hydraulic conductivity for each membrane were determined for each membrane by pumping pure water at deferent operating pressures. the pressure and its corresponding volumetric water flux were recorded. The coefficient of hydraulic conductivity is measured from the slope of a corresponding plot of the volumetric water flux (J_w) as a function of the applied pressure (Δp).

A.2 Sample preparation

In this section an outline of the laboratory procedures used to prepare five litters of PEG 2000. The preparation of other samples follows the same procedures.

A.2.1 Phosphate buffer

All the solutions are buffered using monobasic Potassium salt (KH_2PO_4) as an acid, and dibasic Potassium salt (K_2HPO_4). Equation A.1 is used to estimate the quantities of both the salt and the acid in the solution [18].

$$pH = pK_A + \log\frac{[salt]}{[acid]} \qquad (A.1)$$

where pKA is the minus logarithm of the ionization constant for the acid that equals 7.2. The desired pH for the experimental work is 7.0. Substitute these values in equation A.1 we get

$$7=7.2+\log\frac{[K_2HPO_4]}{[KH_2PO_4]}$$

$[K_2HPO_4]= 0.630\ [KH_2PO_4]$

If the concentration of all phosphate species is 10^{-3}M., then the concentration of each species is:

$[K_2HPO_4]=3.865\times10^{-4}$ M=67.343 mg/l.

$[KH_2PO_4]=6.135\times10^{-4}$. M=83.487 mg/l.

For a five litter solution, the required weights are:

K_2HPO_4= 337mg.

KH_2PO_4= 417 mg.

A.2.2 Polyethylene glycol solution

All experiments are run at a solute concentration of 0.05%, (500 mg/liter). For a five liter solution, the required weight is 2.5 g.

A.2.3 Stock solution preparation

1. Weigh 337 mg of Potassium dibasic phosphate salt (K_2HPO_4) and 417 mg of Potassium monobasic phosphate salt (KH_2PO_4).
2. Dissolve in one liter of pure (MQ) water.
3. Weigh 2.5 g of PEG2000 and dissolve in one liter of (MQ) water.
4. Add the phosphate buffer solution to the PEG solution prepared and dilute to a total volume of 5 liters.
5. Measure the electrical conductivity of the solution and use equation A.2 to calculate the solution ionic strength, I_1 [19].

$$I_1=1.6\times10^{-5}\times EC \qquad (A.2)$$

Where EC is the electrical conductivity of the solution in μ mho/cm.

6. Use equation A.3 to calculate the molarity of Sodium chloride reagent required to adjust the ionic strength of the solution to 0.005 and overall volume of five liters.

$$I = I_1 + I_2 \qquad (A.3)$$

Where I is the desired ionic strength of the solution (0.005), I_1 is the ionic strength of the solution prepared in step four above, I_2 is the ionic strength of sodium chloride solution.

7. Weigh the required amount of NaCl reagent, and dissolve in the solution prepared in step four.

A.3 Sample testing

1. Place the solution in the feed tank (Fig. 6)
2. Release the back pressure valve and turn the pump speed tuner to give the highest speed of the pump.
3. Press the pump button for forward operation.
4. Choke the flow using the back pressure valve such that the pressure gage reading display the desired level of pressure. In this work the pressure difference was 20 psi.
5. Wait until solvent and solute fluxes reach a steady state condition. (15 - 20 minutes).
6. After steady state is attained, take flow measurements and take samples of retentate line, feed tank, and permeate for concentration analysis.
7. Reduce the pumping speed using the pump tuner and adjust the pressure reading to the original value.
8. Repeat steps 5, 6, and 7 above until you collect data for five different pumping speeds for each solution under constant pressure.
9. Repeat steps one to eight for the rest of prepared solutions.

A.4 Membrane washing

The membranes must be washed at the beginning and the end of each run in accordance with the manufacturer recommendations. A solution of 0.1 M solution of NaOH will be applied for 15 minutes and thoroughly rinsed with (MQ) water until no change in the (MQ) water pH is observed. All membranes will be stored wet in a solution of 0.2% Sodium Azide in dark and refrigerator (manufacturer catalog).

APPENDIX B

EXPERIMENTAL RESULTS

Table B.1. Experimental results for pure water flux and pressure.

Pressure (psi)	Pressure (dyn/cm^2)	Volume (ml)	Time (sec)	Flux (cm/sec)
0	0	0	0	0
6	4.13 E5	100	142	2.3500E-03
8	5.52 E5	100	114	2.9200E-03
10	6.89 E5	100	86	3.8800E-03
12	8.26 E5	100	71	4.6900E-03
16	1.10 E6	100	57	5.8500E-03
18	1.24 E6	100	50	6.6700E-03
20	!.38 E6	100	48	6.9400E-03

Regression Output:

Constant	0
Std Err of Y Est	0.000215
R Squared	0.9917774
No. of Observations	8
Degrees of Freedom	7
X Coefficient(s)	5.3169E-09
Std Err of Coef.	8.5777E-11

Table B.2. Summary of model parameters.

Solution	Intercept	s_j	Slope	R^2 %
PEG4k	0.2837594	0.43	23259.648	96.5
PEG6k	0.0203057	0.50	20429.028	94.3
PEG8k	- 0.244255	0.56	27060.677	85.9
PEG10k	-0.491127	0.61	26076.012	96.8
PEG12k	-0.645896	0.66	30153.211	98.9

Table B.3. Summary of solutes concentration on the membrane and its ratio to the concentration in the inflow.

PEG4000		PEG6000		PEG8000		PEG10000		PEG12000	
C^*_w mg/l as COD	$\frac{C_w}{C_i}$	C^*_w mg/l as COD	$\frac{C_w}{C_i}$	C^*_w mg/l as COD	$\frac{C_w}{C_i}$	C^*_w mg/l as COD	$\frac{C_w}{C_i}$	C^*_w mg/l as COD	$\frac{C_w}{C_i}$
1495	1.58	1366	1.72	1800	1.92	1825	2.14	2169	2.44
1537	1.62	1414	1.79	1964	2.10	1933	2.27	2239	2.52
1589	1.68	1473	1.86	2018	2.16	1979	2.32	2309	2.60
1621	1.71	1532	1.93	2045	2.18	2119	2.49	2478	2.79
1642	1.73	1545	1.95	2073	2.21	2157	2.53	2536	2.86

*The solute concentration on the wall was calculated using equation 3.2 in this thesis.

Table B 4. Experimental results for PEG 4000.

Qp ml/sec	Qr ml/sec	Qi ml/sec	Jv (cm/sec)	u (cm/sec)	$u^{0.9}$	$Jv/u.^{09}$	Cp mg/l	Cr mg/l	Ci mg/l	E	$\frac{1-E}{E}$	$\ln\{\frac{1-E}{E}\}$
1.25	36.7	37.95	4.17E-3	71.41	46.6	8.95E-5	852	956	948	0.1	8.96	2.19
1.25	33.3	34.55	4.17E-3	64.91	42.76	9.75E-5	876	956	948	0.076	12.2	2.5
1.25	29.4	30.65	4.17E-3	57.44	38.3	1.09E-4	906	956	948	0.044	21.6	3.07
1.25	21.7	22.95	4.17E-3	42.71	29.34	1.42E-4	924	956	948	0.025	38.5	3.65
1.25	16.7	17.95	4.17E-3	33.15	23.36	1.79E-4	936	956	948	0.013	78	4.36

Regression Output:

Constant	0.2837594
Std Err of Y Est	0.1897857
R Squared	0.9647397
No. of Observations	5
Degrees of Freedom	3
X Coefficient(s)	23259.648
Std Err of Coef.	2567.3225

Table B 5. Experimental results for PEG 6000.

Qp ml/sec	Qr ml/sec	Qi ml/sec	Jv (cm/sec)	u (cm/sec)	$u^{0.9}$	$Jv/u.^{09}$	Cp mg/l	Cr mg/l	Ci mg/l	E	$\frac{1-E}{E}$	$\ln\{\frac{1-E}{E}\}$
1.566	41.5	43.06	5.22E-3	80.9	52.14	1E-4	690	798	792	0.128	6.76	1.91
1.566	37.53	39.06	5.22E-3	72.9	47.47	1.1E-4	714	792	792	0.099	9.15	2.21
1.566	31	32.56	5.22E-3	60.81	40.32	1.3E-4	744	792	792	0.061	15.5	2.74
1.533	22.5	24.03	5.11E-3	44.51	30.45	1.68E-4	774	686	792	0.023	43	3.76
1.533	17	18.53	5.11E-3	34	34	2.14E-4	780	792	792	0.152	65	4.17

Regression Output:

Constant	0.0203057
Std Err of Y Est	0.2685093
R Squared	0.9433417
No. of Observations	5
Degrees of Freedom	3
X Coefficient(s)	20429.028
Std Err of Coef.	2890.5743

Table B 6. Experimental results for PEG 8000.

Qp ml/sec	Qr ml/sec	Qi ml/sec	Jv (cm/sec)	u (cm/sec)	$u^{0.9}$	$Jv/u^{.09}$	Cp mg/l	Cr mg/l	Ci mg/l	E	$\frac{1-E}{E}$	$\ln\{\frac{1-E}{E}\}$
1.43	41.0	42.43	4.76E-3	79.81	51.5	9.24E-5	792	948	936	0.154	5.5	1.7
1.39	37.7	39.09	4.63E-3	73.46	47.8	9.69E-5	864	948	936	0.077	12	2.48
1.35	32.3	33.65	4.50E-3	63.09	41.7	1.08E-4	888	948	936	0.053	18	2.89
1.32	29	30.32	4.39E-3	56.75	37.9	1.15E-4	900	948	936	0.038	25	3.21
1.28	20.7	21.98	4.27E-3	40.83	28.2	1.52E-4	912	948	936	0.026	38	3.64

Regression Output:

Constant	-0.244255
Std Err of Y Est	0.3754133
R Squared	0.8079484
No. of Observations	5
Degrees of Freedom	3
X Coefficient(s)	27060.677
Std Err of Coef.	7617.1974

Table B 7. Experimental results for PEG 10000.

Qp ml/sec	Qr ml/sec	Qi ml/sec	Jv (cm/sec)	u (cm/sec)	$u^{0.9}$	$Jv/u^{.09}$	Cp mg/l	Cr mg/l	Ci mg/l	E	$\frac{1-E}{E}$	$\ln\{\frac{1-E}{E}\}$
1.333	41	42.33	4.44E-3	79.72	51.5	8.84E-5	708	852	852	0.169	4.92	1.59
1.333	38.5	39.83	4.44E-3	74.93	48.7	9.13E-5	750	858	852	0.12	7.35	2
1.333	32.5	33.83	4.44E-3	63.45	41.9	1.06E-4	768	858	852	0.099	9.14	2.21
1.333	24.5	25.83	4.44E-3	48.15	32.69	1.36E-4	822	852	852	0.035	27.4	3.31
1.333	18	19.33	4.44E-3	35.71	24.98	!.78E-4	837	852	852	0.018	55.8	4.02

Regression Output:

Constant	-0.491127
Std Err of Y Est	0.2062339
R Squared	0.9684892
No. of Observations	5
Degrees of Freedom	3
X Coefficient(s)	26076.012
Std Err of Coef.	2715.5812

Table B 8. Experimental results for PEG 12000.

Qp ml/sec	Qr ml/sec	Qi ml/sec	Jv (cm/sec)	u (cm/sec)	$u^{0.9}$	$Jv/u.^{09}$	Cp mg/l	Cr mg/l	Ci mg/l	E	$\frac{1-E}{E}$	$\ln\{\frac{1-E}{E}\}$
1.167	40	41.16	3.89E-3	77.64	50.2	7.74E-5	744	900	888	0.16	5.16	1.64
1.167	36.5	37.66	3.89E-3	70.95	46.33	8.39E-5	768	900	888	0.135	6.14	1.87
1.167	33	34.16	3.89E-3	64.25	42.37	9.18E-5	792	888	888	0.108	8.25	2.11
1.167	24.5	25.66	3.89E-3	47.99	32.59	1.19E-4	850	900	888	0.043	22.4	3.11
1.167	18.5	19.66	3.89E-3	36.51	25.48	1.53E-4	870	888	888	0.02	48.3	3.88

Regression Output:

Constant	-0.645896
Std Err of Y Est	0.113434
R Squared	0.9891649
No. of Observations	5
Degrees of Freedom	3
X Coefficient(s)	30153.211
Std Err of Coef.	1822.0238

APPENDIX C

GLOSSARY

$\overline{V}$	molar volume of the species (cm^3/mol).
$\overline{Mn}$	average number molecular weight.
a	membrane's pore radius (cm).
A_c	cross sectional area of the feed channel (cm^2)
A_m	membrane area (cm^2)
amu	atomic mass unit
B_i	an empirical constant termed as the virial coefficient.
C	solute molar concentration (mol/cm^3).
C'_w	concentration of water on the membrane (mol/cm^3).
C_b	solute concentration in the bulk solution (mol/cm^3)
C_f	solute concentration in the feed (mol/cm^3)
C_i	solute concentration in the inflow (mg/liter)
C_p	solute concentration in the permeate (mol/cm^3)
C_r	retentate concentration (mg/liter)
C_w	solute concentration on the membrane (mol/cm^3).
D	diffusion coefficient (cm2/sec)
dG	Gibs free energy of the system (cal).
dP	external pressure imposed on the thermodynamic system ($dyne/cm^3$)
D_w	coefficient of diffusion for water through the membrane (cm^2/sec)
E	solute removal efficiency $= \frac{Ci - Cp}{Ci}$
f	friction factor

j	Chilton - Colburn factor
J_s	solute flux (mol/cm^2. sec)
J_v	solvent volumetric flux (cm/sec)
J_w	water flux (mol/cm^2. sec).
K	coefficient of mass transfer (cm/sec).
K_d	distribution coefficient for the solute.
K_s	solute coefficient of mass transfer (cm/sec)
K_w	global mass transfer coefficient of water (cm/sec)
L_p	coefficient of hydraulic conductivity (cm^3/ dyne. sec)
M	average molecular weight (amu)
N_i	number of moles of species i in the solution.
N_{Re}	The Reynolds number, $\frac{udh\rho}{\mu}$.
N_{Sc}	The Schmidt number, $\frac{\mu}{\rho D}$.
N_{Sh}	The Sherwood number, $\frac{Kdh}{D}$.
P°	vapor pressure of the chemical species at its pure state(dyne/cm^2).
P	Solute permeation coefficient $\frac{Cp}{Cw}$.
Q_i	inflow flow rate (cm^3/sec)
Q_m	mean fluid flow rate along the membrane module (cm^3/sec)
Q_p	permeate flow rate (cm^3/sec)
Q_r	retentate flow rate (cm^3/sec)
R	universal gas constant (cal/mol-deg.K°).
Ro	Reverse osmosis

S	entropy of the system (cal/deg,K°).
t	membrane tourtosity factor
T	temperature of the system in Kelvin (deg,K°).
UF	Ultrafiltration.
u	mean fluid velocity
V	volume of thermodynamic system (cm^3).
V_w	molar volume of water (cm^3/mol).
X_i	mole fraction of species i in the solution

Greek letters

σ_i	The intrinsic rejection factor= $1 - \frac{Cp}{Cw}$
ε	membrane porosity factor
μ	fluid viscosity (g/sec.cm)
μ_i	chemical potential
ω	solute local permeability factor (cm^2/sec)
π	osmotic pressure (dyne/cm^2)
$\Delta\pi$	osmotic pressure gradient across the membrane (dyne/cm^2)
δ	concentration boundary layer thickness (cm)
δ_m	membrane thickness (cm)
ρ	fluid density (g/cm^3)

REFERENCES

1. Bird, R. B., Stewart, W. E., and Lightfoot, E. N. *Transport Phenomena*. New York: John Wiley& Sons, Inc.,1960.

2. Chao, A. C., Tojo, S., "Permeate Quality of Ultrafiltration Process", *ASCE Journal of Environmental Engineering*, Vol. 113, No2, pp 383- 394, April, 1987.

3. Cheryan, M., *Ultrafiltration Handbook*, Lancaster, Pennsylvania: Technomic Publishing Company, Inc.,1986

4. Chilton, T. H., Coulborn, E. I., "Mass Transfer Coefficients", *Industrial and Engineering Chemistry.*, Vol. 26, No 11, pp. 1183 - 1187, November,1934.

5. Ferry, J. D., "Ultrafilter Membranes and Ultrafiltration", *Chemical. Reviews:* Vol.18, No3, pp 373 - 455 ,1936

6. Geankoplis, C. J. *Transport Process and Unit Operation*, Englewood Cliffs, New Jersey: Prentice Hall, 1989.

7. Goldsmith, R. L. "Macromolecular Ultrafiltration with Microporous Membranes", *Ind. Eng. Chem. Fundam.*, Vol.10, No. 1, pp. 113 - 278, 1971.

8. Harriott, P., Hamilton, R. M., "Solid-Liquid Mass Transfer in Turbulent Pipe Flow", *Engineering Science*, Vol. 20, pp. 1073-1078, 1965.

9. Kedem, O. "Water and Salt Transport in Hyperfiltration" In *Reverse Osmosis Membranes Research.*, Lonsdale, H. K. , H. E. Podall (Eds.), New York: Plenum Press, 1972.

10. Kilduff, J., Weber, W. J. "Transport and Separation of Organic Macromolecules in Ultrafiltration Process", *Environmental Science and Technology*, Vol. 26, No. 3, pp. 569-577, March, 1992.

11. Leung, W. F., Probstein, R. F. "Low Polarization in Laminar Ultrafiltration of Macromolecular Solutions", *Ind. Eng. Chem. Fundam.*, Vol.18, No. 3, pp. 274 - 278, 1979.

12. Levine, A. D., Tachobanoglous, G., Asano, T., " Characterization of the Size Distribution in Wastewater: Treatment and Reuse Implications", *Journal WPCF*, Vol. 57, No 7, pp. 805-816, July, 1985

13. Levine, A. D., Tachobanoglous, G., Asano, T., " Particulate Contaminants in Wastewater: A Comparison of Measurement Techniques and Reported Particle Size Distribution", *Fluid/Particle Separation Journal*, Vol. 4, No , pp. 89-106, June, 1991.

14. Logan, B. E., Jiang, Q, "Molecular Weight Distribution of Dissolved Organic Matter", *ASCE Journal of Environmental Engineering*, Vol. 116, No. 6, pp 1046- 1060, December, 1990.

15. Michaels, S. L.," Crossflow Microfilters ins and outs" *Millipore Corp.* Technical report, June, 1991.

16. Probstein, R. F., *Physicochemical Hydrodynamics: an introduction.*, Stoneham, MA: Butterworth Publishers, 1989.

17. Pusch, W. "Concentration Polarization in Hyperfiltration Systems" In *Reverse Osmosis Membranes Research.*, Lonsdale, H. K. , H. E. Podall (Eds.), New York: Plenum press, 1972.

18. Sawyer, C. N., McCarty, P. L., *Chemistry for Environmental Engineers*, New York: McGraw - Hill, Inc., 1967.

19. *Standard Methods for the Examination of Water and Wastewater*, Washington, D. C: APHA, AWWA, WPCF, 1989.

20. Taylor, J. S., Mulford, L. A., Duranceau, S. J. , Barrett, W. M. " Cost and Performance of Membrane Pilot Plant", *Journal AWWA*, Vol. 81, No. 11, pp. 52- 60, November, 1989.

21. Tchobanoglaous, G., Edward D. S. *Water Quality*, Reading, Massachusetts: Addison Wesley Publishing Company, Inc., 1987.

22. Viessman, Jr. W., and Mark. J. H., *Water supply and pollution control*, New York: Harper Collins Publishers Inc, 1985.

23. Weber, Jr. W. J. *Physicochemical Processes for Water Quality Control.*, New York: John Wiley & Sons, 1972.

24. Wentworth, W. E., and S. Jules. L., *Fundamentals of Physical Chemistry.*, Belmont, California: Wadsworth Publishing Company, Inc., 1972.